

## Phonon dispersion curves for transition metals within the embedded-atom and embedded-defect methods

G. Simonelli, R. Pasianot, and E. J. Savino

*Departamento Materiales, CAC, Comisión Nacional de Energía Atómica, Avenue del Libertador 8250, (1429) Buenos Aires, Argentina*

(Received 30 January 1996)

Phonons in bcc Mo, Fe, and Cr have been calculated using embedded-atom-method (EAM)-type and embedded-defect (ED) potentials. The latter is an extension of the EAM that introduces angular interactions through a many-body approach. In contrast with the EAM formalism, the ED calculated elastic constants can be fitted to the experimental values even in those metals with a negative Cauchy pressure. The contributions of the pair and many-body interaction terms to the phonon frequencies are studied. It is found that the EAM and ED interatomic potentials show some limitations to reproduce the experimental dispersion curves for bcc and fcc structures; such limitations are analyzed. [S0163-1829(97)04610-9]

### I. INTRODUCTION

Even nowadays, with large memory and high-speed computers available, relatively simple semiempirical interatomic potentials are mostly used for the simulation of extended defects in crystal solids. In the past decade, the fast running pair interaction potential, used almost exclusively in the 60's and 70's, has been superseded by simple many-body approaches, called generically either embedded-atom-method<sup>1</sup> or Finnis and Sinclair potentials<sup>2</sup> (EAM hereafter). Those interaction models still retain the computational simplicity of the pair one but solve some of its limitations, i.e., the fitting of the elastic constants in equilibrium for most metals, the different values of cohesive and vacancy formation energies, and the free surface relaxation. However, the angle-dependent part of the atomic interactions is not included, either in the pair or in those many-body potentials. Some aspects of angle-dependent bonding are already reflected in the elastic behavior of monatomic metals; for instance, the measured negative value of the Cauchy pressure  $(c_{12} - c_{44})/2$  in Cr (Ref. 3) cannot be fitted within the EAM formalism. To solve this limitation, other interatomic potentials were derived from the EAM.<sup>4-8</sup> Among them, the embedded-defect (ED) model was developed<sup>5</sup> and applied to the calculation of point defects in Fe.<sup>9,10</sup>

Empirical or semiempirical potentials are generally fitted to a limited number of crystal data (lattice parameter, cohesive energy, elastic constants, some defect formation energies, etc.); however, one expects to attain a correct prediction of the properties that, somehow, depart from this parameter space. Perhaps the easiest test of dynamical properties is the phonon dispersion curves calculation, for which there is a large base of experimental measurements. This is seldom done in the papers where EAM potentials are developed and phonon frequencies are rarely taken as fitting parameters,<sup>11</sup> in spite of the suggestion in Refs. 12 and 13. This point will be discussed further in this report.

In the present work, phonon dispersion curves for Mo, Fe, and Cr are calculated using ED and EAM-type potentials developed as discussed in Refs. 5, 9, and 10. The contributions of the different terms in the interaction to the phonon

frequencies are separated. The calculated curves are compared with experimental results. Some general limitations in obtaining a correct fitting to experiments in bcc and fcc materials are derived.

### II. PHONON DISPERSION CURVES

Within the ED method proposed in Ref. 5, the energy  $E_i$  at atomic site  $i$  is expanded as

$$E_i = \frac{1}{2} \sum_{j \neq i} V(R_{ij}) + F(\rho_i) + G(Y_i). \quad (1)$$

The first term  $V(R_{ij})$  represents a pair interaction, it is a function of the distance  $R_{ij}$  between atoms  $i$  and  $j$ , while the many-body character is contained in the terms  $F(\rho_i)$  and  $G(Y_i)$ . The arguments  $\rho_i$  and  $Y_i$  are calculated using a tensor function  $\bar{\kappa}$  defined at each atomic site

$$\lambda_i^{\alpha\beta} = \sum_{j \neq i} \Phi(R_{ij}) R_{ij}^\alpha R_{ij}^\beta / R_{ij}^2, \quad (2)$$

where  $\alpha$  and  $\beta$  are Cartesian components, and  $\Phi$  is a function of the distance  $R_{ij}$ . Then,

$$\rho_i = \text{Tr} \bar{\kappa}_i = \sum_{j \neq i} \Phi(R_{ij}) \quad (3)$$

and

$$Y_i = \sum_{\alpha, \beta} \lambda_i^{\alpha\beta} \lambda_i^{\alpha\beta} - \rho_i^2 / 3. \quad (4)$$

Thus,  $F$  is analogous to the so-called "embedding function" of the EAM (Refs. 1 and 2) and  $G$  results sensitive to angular distortions. Our EAM potential results from applying Eq. (1) with  $G=0$ . We define  $V(R_{ij})$  as an "effective pair" equilibrium interaction potential; as proved in Ref. 2, this can always be done for any EAM potential. Also, for the ED potential, the first two terms of Eq. (1) constitute an "effective EAM potential;" i.e., it is an EAM potential which would simulate a metal with the same lattice parameter than the one of interest, but certainly with different shear moduli

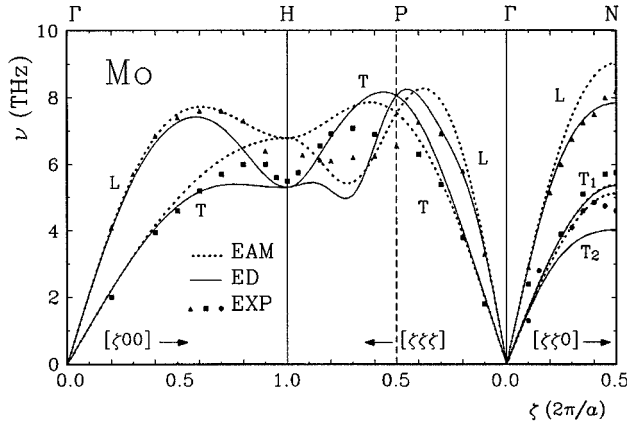


FIG. 1. Phonon dispersion curves for Mo calculated with our EAM and ED potentials.  $\nu = \omega/2\pi$  vs  $\mathbf{k}$  are plotted. Experimental points are from Ref. 19.

and vacancy formation energy, since these properties do also have a contribution from angular term  $G$ .<sup>5</sup> This gauging enables the calculation of the contributions by the different terms in Eq. (1) to the dynamical properties. Within the ED model, the many-body contribution to  $E_f^{vNR}$  remains as a free parameter;<sup>5</sup> here, for consistency, it is fixed as 20% for all the simulated metals. EAM and ED potentials for Fe were discussed in detail in Refs. 9 and 10. The ones for Mo and the ED potential for Cr have been developed by following the same parameter fitting procedure. They are fitted to the equilibrium lattice parameter  $a$ ,<sup>14</sup> to the cohesive energy  $E_{\text{coh}}$ ,<sup>15</sup> to the vacancy formation energy  $E_f^v$ ,<sup>16,17</sup> and to the three elastic constants.<sup>18,3</sup>

The phonon dispersion curves are calculated by solving the eigenvalues  $\omega(\mathbf{k})$  of the dynamical matrix, along some high symmetry directions of the Brillouin zone. The resulting curves are presented in Figs. 1–3, together with the experimental points. It may be seen that both the EAM and the ED potentials duplicate the experimental results for the reciprocal lattice vector  $\mathbf{k} \rightarrow 0$ , as it is expected from their exact fitting to the elastic constants. In general, the ED potentials

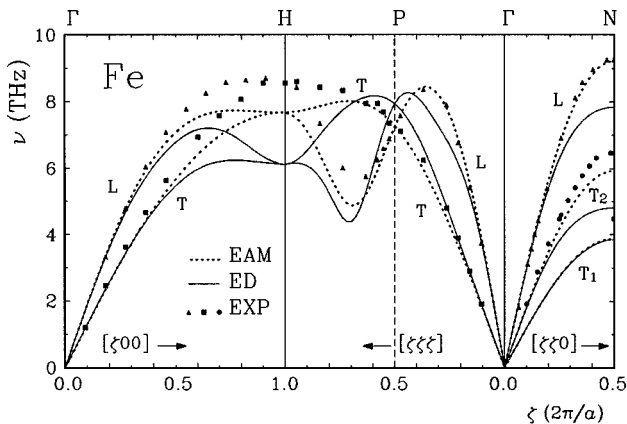


FIG. 2. Same as Fig. 1, for Fe. Experimental points are from Ref. 20.

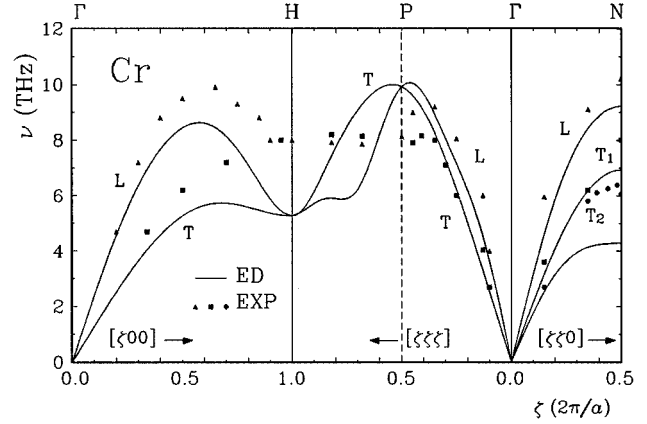


FIG. 3. Phonon dispersion curves for Cr calculated with the ED potential. Experimental data are from Ref. 21.

predict lower longitudinal ( $L$ ) frequencies than the EAM ones and they also do so for transverse ( $T$ ) modes in some regions of the spectrum. This is advantageous when ED is used to reproduce the experiments in Mo, where a frequency softening at point  $H$  [ $\mathbf{k} = (2\pi/a)(100)$ ] has been measured. Actually, for this metal, a good agreement is found all over the zone in the  $[100]$  direction (including point  $H$ ) between the frequencies calculated with the ED and the ones measured. However, for Fe, the mentioned softening is not found and the EAM potential reproduces experimental results better than the ED one. Consequently, we conclude that better fittings to phonon dispersion measurements are obtained by using an ED interaction potential for Mo and an EAM one for Fe.

As discussed in Ref. 5 and above, the ED potential has been developed especially to enable the fitting of elastic constants in the case of a negative Cauchy pressure, such as in Cr. Although the ED solves this problem, we find that, for Cr, the agreement between measured and calculated phonon dispersion curves is not good for this potential, see Fig. 3. Causes for this lack of fitting are discussed in Sec. III.

Figure 4 shows a calculation performed for Mo, where the

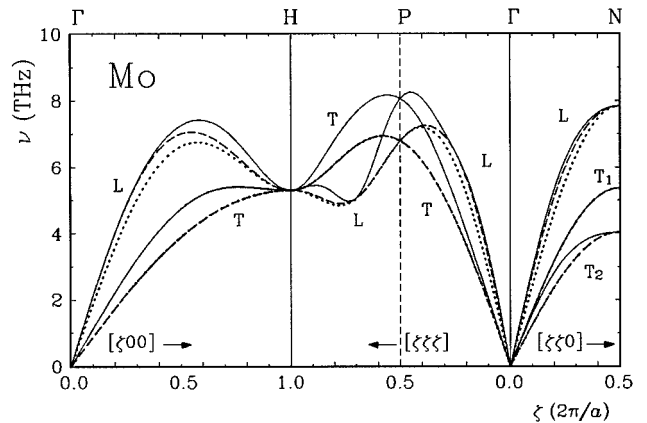


FIG. 4. Phonon dispersion curves for Mo with the ED potential, where successive terms of Eq. (1) are added: (a)  $\cdots$  only the pair interaction  $V$  is considered, (b)  $---$   $V$  and the embedding function  $F$  are considered for the calculation, and (c) — complete ED potential.

TABLE I. Quantity in the first column for several transition metals (see text). Between brackets, the values obtained replacing  $c_{44}$  by  $c_{44\text{pair}}$  corresponding to the ED potentials.

bcc	Fe	Mo	Cr	W	V	Nb	Ta
$\frac{12\Omega c_{44}}{MR_1^2 \omega_H^2} - 1$	-0.01 (-0.34)	0.49 (-0.07)	0.10 (-0.41)	0.22	-0.50	-1.42	-0.26
fcc	Cu	Ag	Au	Ni	Pd	Pt	
$\frac{8\Omega c_{44}}{MR_1^2 \omega_x^2} - 1$	0.07	0.04	-0.24	0.25	-0.26	-0.36	

terms in the ED potential of Eq. (1) are added successively [i.e., the dispersion curves are calculated by using: (a) the ‘‘effective pair’’ potential, (b) the ‘‘effective EAM’’ one, defined above, and (c) the whole ED]. A salient feature is that the (spherically symmetric) term  $F$  does not contribute to  $T$  branches and that only the pair term contributes to the frequencies at zone boundaries  $H$  (where  $T$  and  $L$  coincide) and at  $N$ . Evidently, these are also general results for EAM-type potentials. The negligible participation of term  $G$  in  $T1$  is consistent with its small contribution to the shear modulus  $(c_{11} - c_{12})/2$ .<sup>5</sup> On the other hand, the contribution to  $T2$ , associated to  $c_{44}$ , is significant. We also found that the major effect of introducing  $G$  is that the calculated phonon frequency at point  $P$  is raised; this effect does not help the fitting of the measured values in any of the cases studied here (see Figs. 1–3).

### III. DISCUSSION

The fact that, at point  $H$ , only the pair-term contributes to the phonon frequencies can be exploited to obtain some analytic relationships, within our interaction models, between elastic constants and frequencies. Assuming that the pair interaction reaches up to second neighbors, the expression for the frequency at point  $H$  is

$$M \omega_H^2 = \frac{16}{3} \left( V_1'' + 2 \frac{V_1'}{R_1} \right), \quad (5)$$

where  $V_1'$  and  $V_1''$  are, respectively, the first and second derivatives at the first neighbors' distance  $R_1$ . In turn, the contribution to  $c_{44}$  coming from the equilibrium pair term is

$$\Omega c_{44\text{pair}} = \frac{4}{9} (R_1^2 V_1'' - R_1 V_1'), \quad (6)$$

$\Omega$  being the atomic volume. The many-body part imposes an extra positive contribution to reach the experimental value of  $c_{44}$ . However, shear moduli do not depend on the density  $\rho$  (see Ref. 5) and, therefore,  $c_{44\text{pair}}$  differs from the experimental value only for the ED potential. As for any feasible functional shape  $V_1'' > 0$  and  $V_1' < 0$ , the following inequalities are obtained:

$$\omega_H^2 \leq \frac{12\Omega c_{44\text{pair}}}{MR_1^2} \leq \frac{12\Omega c_{44}}{MR_1^2}. \quad (7)$$

A similar relationship is obtained for the frequency of the  $T$  mode at  $\mathbf{k} = (2\pi/a)(100)$  (point  $X$ ) for an fcc structure, in which 12 is replaced by 8. In Table I, quantity  $(12\Omega c_{44})/(MR_1^2 \omega_H^2) - 1$  is reported for the bcc transition metals, while the corresponding one is reported for some fcc transition elements. A negative value means that no EAM can fit both  $c_{44}$  and  $\omega_{\mathbf{k}=(2\pi/a)(100)}^2$ ; this is so for V, Nb, Ta, Au, Pd, and Pt in Table I. In those cases, for the ED potentials, the situation is still worse, because the corresponding  $c_{44\text{pair}}$  is smaller (see Table I). In turn, a positive value for the above quantity indicates that a fit employing either EAM or ED may result successful. In the case of Cr, where only ED can be fitted to the negative Cauchy pressure, the value obtained in Table I is positive; however, the weight of the angular term is so large that the first inequality of Eq. (7) cannot be fulfilled (see Table I). On the other hand, in Fe, the relatively small negative value allows a reasonable (although not exact) fitting when the EAM potential is used.

The softening of the  $L$  branches in Mo and Cr has been attributed to electron-phonon interactions.<sup>19</sup> In our ED potential model, this softening is a consequence of constraining the potential to reproduce the experimental elastic constants (and, therefore, the slopes at point  $\Gamma$ ), which, in the fitting procedure reduces the value of  $c_{44\text{pair}}$ . This, in turn, according to Eq. (7), lowers the maximum achievable value of  $\omega_{\mathbf{k}=(2\pi/a)(100)}^2$ . Also,  $G(Y)$  increases  $\omega_{\mathbf{k}=(\pi/a)(100)}^2$  and, therefore, the difference with the value at  $H$ .

Foiles<sup>8</sup> has considered angular terms based on the fourth moment of the electronic density of states similar to Carlson's method.<sup>6</sup> The author performed phonon calculations for Mo and W and found that, by increasing the energetic contribution of those terms, some zone-edge phonon frequencies decreased. He concluded that the fitting of the experimental phonon frequencies spectra was not improved by his extended method with respect to the EAM.

Calculations with EAM potentials, with pair interactions ranging up to second neighbors,<sup>12,13,22</sup> are consistent with our prediction that the resulting phonon frequencies for Nb, V, and Ta, among the bcc transition metals, and for Pt, Pd, and Au, among the fcc ones, are larger than the measured values. We conclude that for some metals, within the EAM, a proper fit cannot be obtained to both the elastic constants and to the phonon frequencies at  $H$  ( $X$  for fcc). This opposes the expectations of Refs. 12 and 13, where it is claimed that, by means of a careful choice of fitting parameters of the EAM functions, the agreement with experimental dispersion curves

could be improved considerably without spoiling other fittings. Actually, one may consider that the restriction in deducing Eq. (7) for up to second-neighbor interactions is causing this limitation, however, this does not seem to be the case; in fact calculations with EAM potentials reaching beyond second neighbors<sup>23,24</sup> provide results in the direction we point for almost all the transition metals considered in Table I.

## ACKNOWLEDGMENTS

This work was supported by Consejo Nacional de Investigaciones Científicas y Técnicas (CONICET) and Proyecto Multinacional de Materiales (Organización de Estados Americanos—Comisión Nacional de Energía Atómica, PMM OEA-CNEA), Argentina.

- 
- <sup>1</sup>M. S. Daw and M. I. Baskes, *Phys. Rev. B* **29**, 6443 (1984).  
<sup>2</sup>M. W. Finnis and J. E. Sinclair, *Philos. Mag. A* **50**, 45 (1984); **53**, 161 (1986).  
<sup>3</sup>H. J. van Rijn and H. L. Alberts, *J. Phys. F* **13**, 1559 (1983).  
<sup>4</sup>M. I. Baskes, J. S. Nelson, and A. F. Wright, *Phys. Rev. B* **40**, 6085 (1989).  
<sup>5</sup>R. Pasianot, D. Farkas, and E. J. Savino, *Phys. Rev. B* **43**, 6952 (1991); **47**, 4149 (1993).  
<sup>6</sup>A. E. Carlsson, *Phys. Rev. B* **44**, 6590 (1991).  
<sup>7</sup>M. I. Baskes, *Phys. Rev. B* **46**, 2727 (1992).  
<sup>8</sup>S. M. Foiles, *Phys. Rev. B* **48**, 4287 (1993).  
<sup>9</sup>G. Simonelli, R. Pasianot, and E. J. Savino, *Phys. Rev. B* **50**, 727 (1994).  
<sup>10</sup>G. Simonelli, R. Pasianot, and E. J. Savino, *Phys. Status Solidi B* **191**, 249 (1995).  
<sup>11</sup>J. M. Eridon, in *Atomistic Simulation of Materials*, edited by V. Vitek and D. J. Srolovitz (Plenum, New York, 1989), p. 211.  
<sup>12</sup>M. S. Daw and R. D. Hatcher, *Solid State Commun.* **56**, 697 (1985).  
<sup>13</sup>R. Rebonato and J. Q. Broughton, *Philos. Mag. Lett.* **55**, 225 (1987).  
<sup>14</sup>*American Institute of Physics Handbook* (McGraw-Hill, New York, 1957).  
<sup>15</sup>C. Kittel, *Introduction to Solid State Physics*, 5th ed. (Wiley, New York, 1976).  
<sup>16</sup>K. Maier, M. Peo, B. Saile, H. E. Schaefer, and A. Seeger, *Philos. Mag. A* **40**, 701 (1979).  
<sup>17</sup>G. D. Loper, L. C. Smedskjaer, M. K. Chason, and R. W. Singru, *Positron Annihilation*, edited by P. C. Jain, R. M. Singru, and K. P. Gopinathan (World Scientific, Singapore, 1985), p. 461.  
<sup>18</sup>G. Simmons and H. Wang, *Single Crystal Elastic Constants and Calculated Aggregate Properties: a Handbook*, 2nd ed. (MIT Press, Cambridge, MA, 1971).  
<sup>19</sup>A. D. B. Woods and S. H. Chen, *Solid State Commun.* **2**, 233 (1964).  
<sup>20</sup>V. J. Minkiewicz, G. Shirane, and R. Nathans, *Phys. Rev.* **162**, 528 (1967).  
<sup>21</sup>H. B. Møller and A. R. Mackintosh, in *Inelastic Scattering of Neutrons* (International Atomic Energy Agency, Vienna, 1965).  
<sup>22</sup>A. M. Guellil and J. B. Adams, *J. Mater. Res.* **7**, 639 (1992).  
<sup>23</sup>J. B. Adams and S. M. Foiles, *Phys. Rev. B* **41**, 3316 (1990).  
<sup>24</sup>F. Cleri and V. Rosato, *Phys. Rev. B* **48**, 22 (1993).